Korean J. Chem. Eng., 33(9), 2756-2760 (2016)
DOI: 10.1007/s11814-016-0093-7

pISSN: 0256-1115
eISSN: 1975-7220

A novel rapid mist spray technique for synthesis of single phase precipitated calcium carbonate using solid-liquid-gas process

Jimoh Abdullateef Onimisi[*,], Roniza Ismail[*], Kamar Shah Ariffin[*,†], Norlia Baharun[*], and Hashim Bin Hussin[*]**

*School of Materials and Mineral Resources Engineering, Universiti Sains Malaysia, 14300 Nibong Tebal, Penang, Malaysia
**Department of Geology, Federal University Lokoja, Nigeria

(*Received 26 January 2016 • accepted 31 March 2016*)

Abstract−Various techniques and approaches have been designed to synthesize precipitated calcium carbonate. We used a continuous sprayed-mist technique that induced spontaneous precipitation reaction of the droplets with the higher surface area when in contact with the gas. The effects of optimum reactant concentration, gas flow rate, and reactant feeding rate including reaction conditions were investigated. The effectiveness of the techniques was scrutinized by analyzing the resultant PCC characteristics, especially the particle phase morphology and size distribution using XRD, FTIR, and SEM. The variation of initial concentration of milk of lime with different gas flow rate was studied. Experimental results, as well as XRD and FTIR, indicated that all the products produced were favorable for the formation of calcite. SEM revealed that the morphologies of PCC were all rhombohedral and tended to adhere to each other (twinning). It was found that production of PCC by using spray-mist method is suitable for lower initial concentration of $Ca(OH)_2$ and higher gas flow rate only.

Keywords: Precipitated Calcium Carbonate (PCC), Spray Mist, Continuous, Calcite, Gas-flow

INTRODUCTION

Precipitated calcium carbonate (PCC) is the preferred filler used in many applications like paper making, plastics, rubbers, paints, drugs and so on. Its high purity and close controlled particle size and shape make it the white filler of choice. PCC in recent years has gained commendable attention in filler industries as one of the cheapest and best available fillers commercially [1,2]. The application of calcium carbonate particles is mainly determined by the polymorphs of $CaCO_3$. Calcium carbonate has three crystal polymorphs: rhombic calcite, needle-like aragonite and spherical vaterite [3]. Calcite is the most stable phase at room temperature under normal atmospheric conditions, while aragonite and vaterite are metastable polymorphs that readily transform into the calcite stable phase [4-6]. Morphology of PCC can be influenced by the use of additives either in carbonation route or solution reaction route [7]. Kim et al. [8] used aspartic acid to influence the morphology of PCC. Similarly, Stroescu et al. [9] reported the change in PCC morphology when sodium dodecyl sulfate (SDS) and cetyltrimethylammonium bromide (CTAB) was utilized. Song et al. [10] also reported the influence of lysozyme and aspartic acid on the morphology and particle size of PCC. However, the adsorption of additives at solid-liquid interface is profoundly essential for various technical applications [11]. Particle size distribution and polymorph of calcium carbonate formed during synthesis are subjected to supersaturation level and the ionic ratio of the reactant in the solution [12].

Over the years, many techniques have been designed to synthesize specific quality of PCC in order to meet many downstream application specifications. The most widely used method to obtain PCC at industrial scale is the carbonation route, which consists of bubbling CO_2 gas through an aqueous slurry of slaked lime (a $Ca(OH)_2$ suspension) in a batch process [13-15]. Basically, it consists three steps of preparing PCC in the industrial procedure [16, 17]:

(a) calcinations of the calcitic limestone
$CaCO_3\ (s) \rightarrow CaO\ (s) + CO_2\ (g)$

(b) slaking process
$CaO\ (s) + H_2O\ (l) \rightarrow Ca(OH)_2\ (l)$
(c) recarbonation
$Ca(OH)_2\ (l) + CO_2\ (g) \rightarrow CaCO_3\ (s) + H_2O\ (l)$

As the reaction (carbonation) proceeds, a reduction in the concentration of ions is present and this can be monitored by the measurement of conductivity of the suspension. Also, the use of the hydroxyl ions from the calcium hydroxide dissociation for the calcium carbonate production allows the study of the reactive process on the basis of the pH value [18]. It was observed that the pH of the suspension is the most important factor affecting the polymorphs of calcium carbonate [19]. Synthesizing PCC with precise morphology and particle size is, however, difficult in the carbonation process using traditional batch reactor [20].

In this work, sprayed mist technique was utilized to synthesize PCC. The lime slurry was introduced continuously into the reactant chamber as fine liquid droplets under high pressure together with the CO_2 gas. Such situation created a cloudy environment rich with the milk of lime vapors with high surface area. This led to a better exposure and spontaneous reaction of the reactant with the gas, thus PCC formation with specific polymorph. Our aim here

---

[†] To whom correspondence should be addressed.

E-mail: kamarsha@usm.my

was to give an insight into the influence of sprayed mist technique on the production of PCC and the properties of the particles formed.

EXPERIMENTAL PROCEDURE

1. Preparation of Reactant

High purity limestone was crushed into manageable size range of 10-20 mm diameters before being calcined in the muffle furnace at 1,100 °C for 90 minutes. The resulting quicklime was then hydrolyzed with distilled water to produce calcium hydroxide. Then, the suspension was screened to remove any coarse grits and impurities to below 75 μm prior to experiments. As shown in Table 1, the experiments were conducted at a few variety concentration of the reactant like 0.1 M, 0.14 M, 2 M and 2.5 M to study the effect of concentration of reactant using this technique.

2. Carbonation Process in Sprayed Mist Technique

The experiments were run in a spray mist reactor that was initially filled with CO_2 gas; subsequently, the reactant $Ca(OH)_2$ was introduced to make an effective carbonation process. At the same time, the reactant in the feed container was stirred by a magnetic stirrer to make sure the suspension was homogeneous before the feed passed through the spray gun. Immediately after gas was supplied into the reactor, $Ca(OH)_2$ was introduced into the reactor chamber as fine liquid droplets through the spray gun under high pressure together with the gas continuously. As, higher velocity will deliver slurry particles more uniformly into reactant chamber [21]. The $Ca(OH)_2$ mists that were produced reacted with CO_2 gas in the reactor for the precipitation process. The height of the reactor enabled ample exposure of $Ca(OH)_2$ mist in the reaction. As the mist dropped at the base of the reactor, it accumulated as a

Table 1. Experimental conditions and results on the changes of pH, conductivity and temperature measured before and after the carbonation (via spray mist technique)

Experiment	Reactant concentration (M)	Gas flow rate (ml/min)	pH		Conductivity (mS/cm)		Temperature	
			Initial	Final	Initial	Final	Initial	Final
SPCC A1	0.1	898.1	11.89	6.52	8.22	0.994	28.9	24.9
SPCC A2	0.1	1121.8	11.89	6.91	8.22	0.492	28.9	25.6
SPCC A3	0.1	5000	11.71	6.72	8.39	1.022	28.6	24.1
SPCC B1	0.14	898.1	12.01	9.15	8	0.062	28.6	26.5
SPCC B2	0.14	1121.8	12.01	6.94	8	0.572	28.6	26
SPCC B3	0.14	5000	11.71	6.73	8.35	0.561	28.5	23.6
SPCC C1	0.2	898.1	11.78	11.63	8.69	7.64	29.3	26.3
SPCC C2	0.2	1121.8	11.83	8.68	8.24	0.188	29.2	25.8
SPCC C3	0.2	5000	11.71	6.98	8.3	0.74	29.3	25.7
SPCC D3	0.25	5000	11.8	7.45	8.69	0.37	28.3	24.1

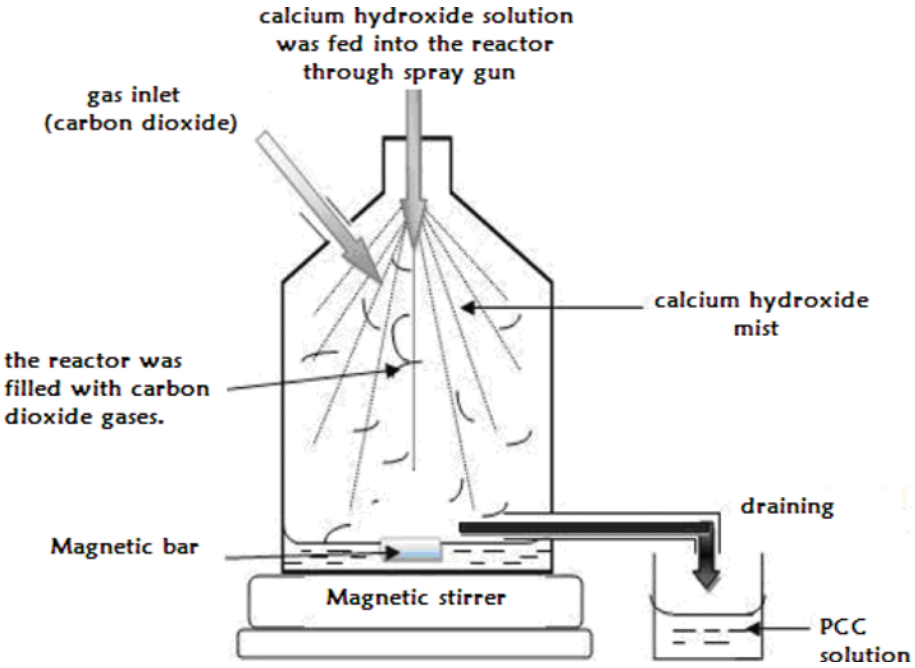

Fig. 1. Spray mist reactor used to synthesize the PCC particles.

suspension before coming out through the drain outlet which was located at a height of 1cm from the base. Stirring involved using a magnetic bar at the base to mix the suspension properly and ensure complete reaction (Fig. 1). Initial and final pH, conductivity and temperature values, respectively, were obtained using a TPS pH meter. The pH value was taken before and after the carbonation process. Initially, the pH value of the reactant was measured and, usually, the pH was or approximately 12 at the beginning. Once the reactant passed the precipitation reactor and out from the reactor, the product, which was the PCC solution, was measured to see the changes of the pH value. The neutral pH value indicated the reaction was completed and indicated there was no more excess Ca_2^+. All the experiments stopped at the nearly same pH value.

For the conductivity value, the reading could not be related obviously for all the experiments, as the value for initial and final were quite similar, which is around 8 mS/cm and less than 1 mS/cm, respectively. But for SPCC C1, the final value was not much different from the initial as the value decreased just a little bit and not less than 1 mS/cm compared to other experiments. This showed that the precipitation process was totally incomplete (see Table 1).

3. Characterization

At the end of the experiment, the final precipitates were washed with distilled water, filtered and dried at 105 °C for 24 hours to eliminate the water. Morphological analysis of the PCC's products was performed by scanning electron microscopy (SEM). The X-ray diffraction (XRD) was obtained using a Bruker D8 Advance X-ray powder diffractometer with filtered Cu-Kα radiation (λ=1.542) operating at a beam voltage and current of 40 kV and 40 mA, respectively. The XRD patterns were recorded in the range of $2\theta=5^{\circ}$-90° using a step size of 0.034° and scan step time of 71.6 seconds was used for all analysis to identify the phase composition of the samples. The infrared spectra of the samples dispersed in KBr pellets were recorded using Perkin Elmer FTIR spectrometer.

RESULTS AND DISCUSSION

In sprayed mist technique, the reactant ($Ca(OH)_2$) was converted to fine mists, which tremendously increased the surface area of the reactant. Due to the high surface area that occurs in the fine mists, the carbon dioxide gas reacted with Ca^{2+} ions enhancing quick precipitation of PCC. The carbonation reaction is shown below:

$$Ca(OH)_2 \text{ (liquid in mists form)} + CO_2 \text{ (gas)} \rightarrow CaCO_3 \text{ (liquid)}$$

During the experiment, decrease in temperature from 28 °C to 23 °C was observed (as shown in Table 1).The decrease in temperature for each experiment showed that spray mist technique gives a cold situation to this process as the reactant was introduced as a fine mist that created a cloudy environment in the reactor. And at the same time, CO_2 gas was a cold gas supplied in high flow rate, thereby affecting the temperature.

SEM observations in all the samples showed that the morphology of PCC samples did not change obviously with the major view of plate-like rhombohedral calcite. Some of the rhombohedral particles attached to each other and formed a layer of $CaCO_3$ plates as a result of twinning, which is a crystal growth disorder. This result indicates that lower temperature synthesis favors the aggregation of the calcite crystals due to low energy points on the surface of the reaction.

As shown in Fig. 2(a), SPCC A1 with 0.1 M concentration at 898.1

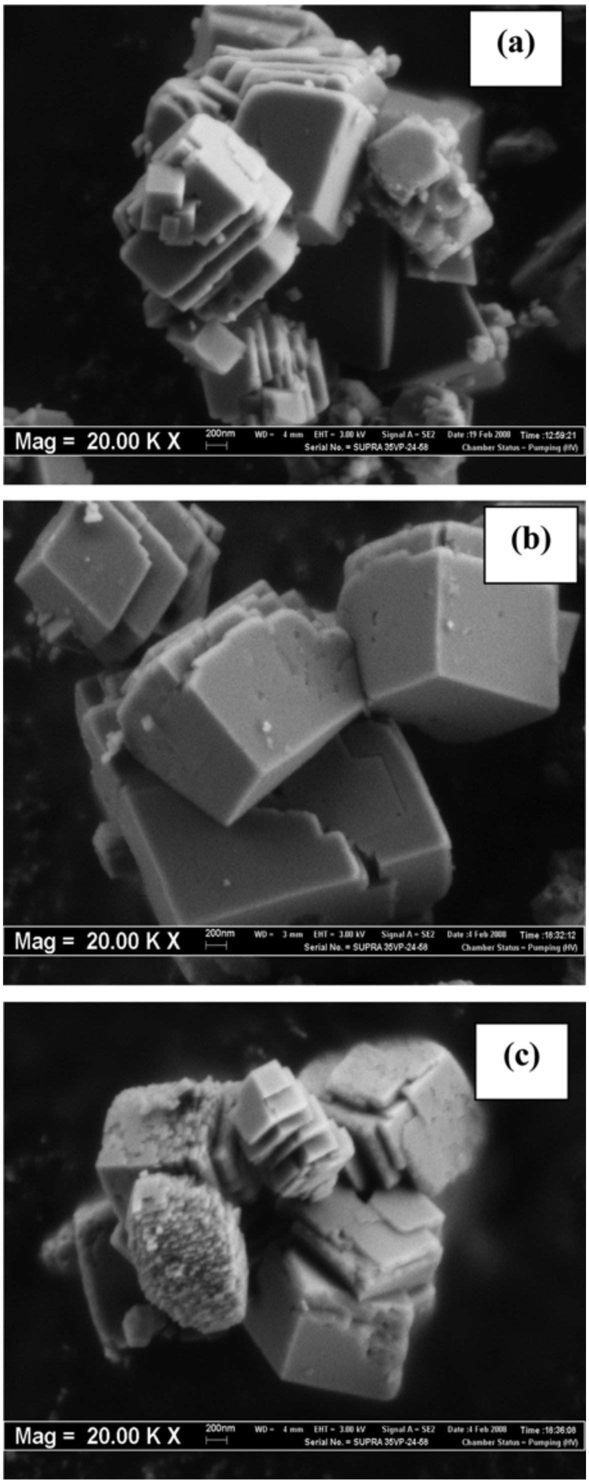

Fig. 2. Variation in the rhombohedra calcite surface morphology precipitated at different reactant concentrations and gas flow rate, (a) 0.1 M concentration at 898.1 ml/min gas flow (b) concentration of 0.2 M and 1,121.8 ml/min gas flow rate (c) 0.2 M higher gas flow rate of 5,000 ml/min.

ml/min gas flow rate, the aggregated rhombohedral calcite particles present well-defined plate-like edges with a crystal size of 30 nm to 400 nm. On the other hand, the surface and edges of rhombohedral calcite for SPCC C2 with increased concentration of 0.2 M and 1,121.8 ml/min gas flow rate (Fig. 2(b)) is seen to be rough with few lines of breakage. Further increase in gas flow rate to 5,000 ml/min in sample SPCC C3 (Fig. 2(c)) yielded a highly corroded rhombohedral calcite surface. However, the structures were observed to be similar to sample SPCC C2. Fig. 3 shows SEM micrographs for three samples which were prepared at different reactant concentrations (0.1 M, 0.2 M and 0.25 M), SPCC A3, SPCC C3 and SPCC D3, respectively, but at the same CO_2 gas flow rate (5 L/min) to see the effect of concentration on each morphology. It can be seen that there was slight decrease in particle size decrease when the reactant concentration increase.

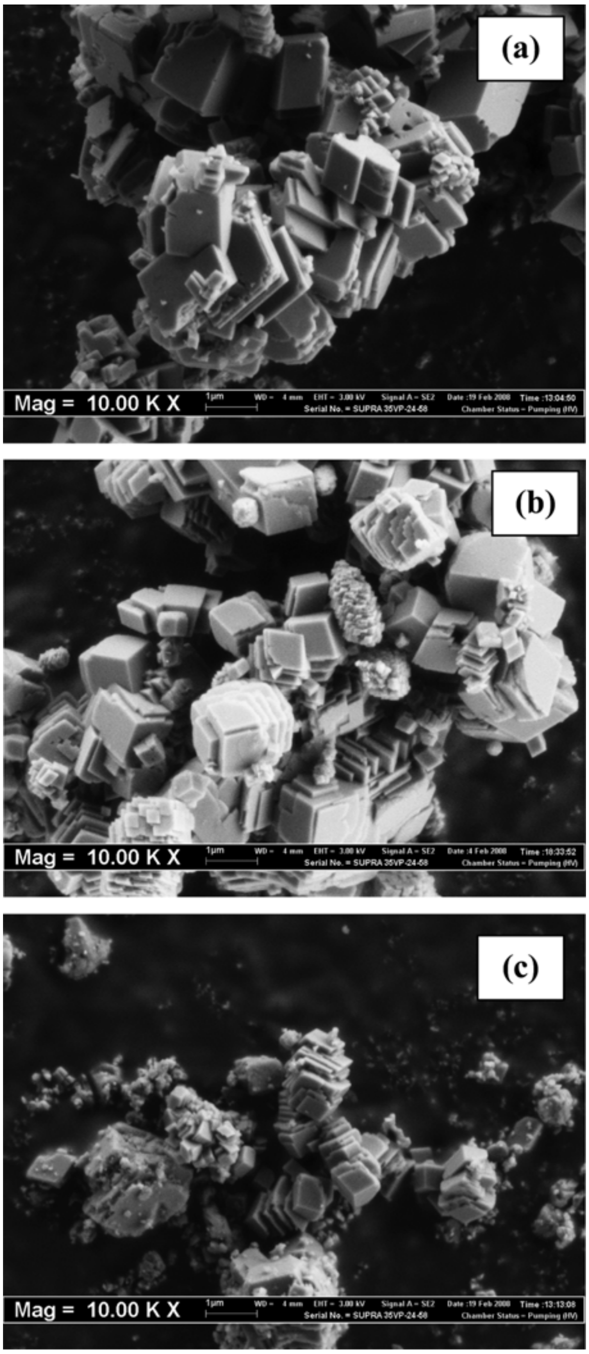

Fig. 3. SEM micrographs of PCC precipitated at gas flow rate of (5 L/min) at different concentration of reactants (a) 0.1 M (b) 0.2 M (c) 0.25 M.

It is deduced that lower reactant concentration and the higher CO_2 gas flow rate at ambient temperature by using spray mist technique may provide a favorable condition for the formation of twinned rhombohedral calcite.

FTIR was used to identify the chemical bonding structure of molecules and it was useful to analyze the crystal morphology. FTIR identifies chemical bonds in a molecule by producing an infrared absorption spectrum. The FTIR spectrum contained absorption peaks at 1,798, 1,425, 876 and 713 cm^{-1} which were assigned to the CO_3^{2-} (as shown in Fig. 4). FTIR spectra of $CaCO_3$ polymorphs display characteristic absorption bands in the region 1,850-650 cm^{-1} corresponding to the four types of C-O bond vibrations, namely symmetric stretching (v_1), out-of-plane bonding (v_2), a doubly degenerate asymmetric stretching (v_3) and a doubly degenerate in-plane bonding (v_4). The symmetric stretching mode v_1 is infrared inactive, hence, only three bands due to v_2, v_3 and v_4 are observed in the FTIR spectrum of calcite at 876, 1,425 and 713 cm^{-1} respectively. According to [22], the IR absorption bands at 1,423, 877 and 712 cm^{-1} were attributed to a Ca-O stretching and bending vibrations, respectively. The little difference of absorption bands showed that the formed PCC have somewhat variation in crystal morphology or atomic structure during precipitation.

X-ray diffraction (XRD) was used to characterize the phase of the precipitates sampled. The lattice parameters were evaluated ac-

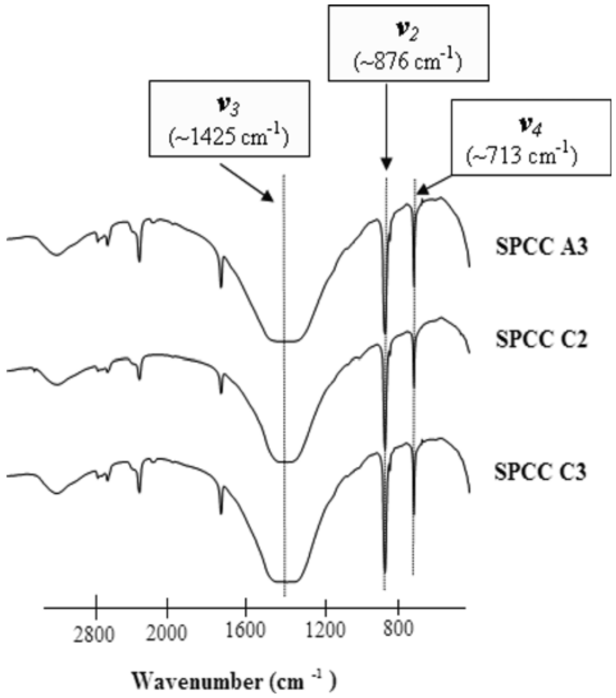

Fig. 4. FTIR spectra of PCC samples for SPCC A3, SPCC C2, and SPCC C3.

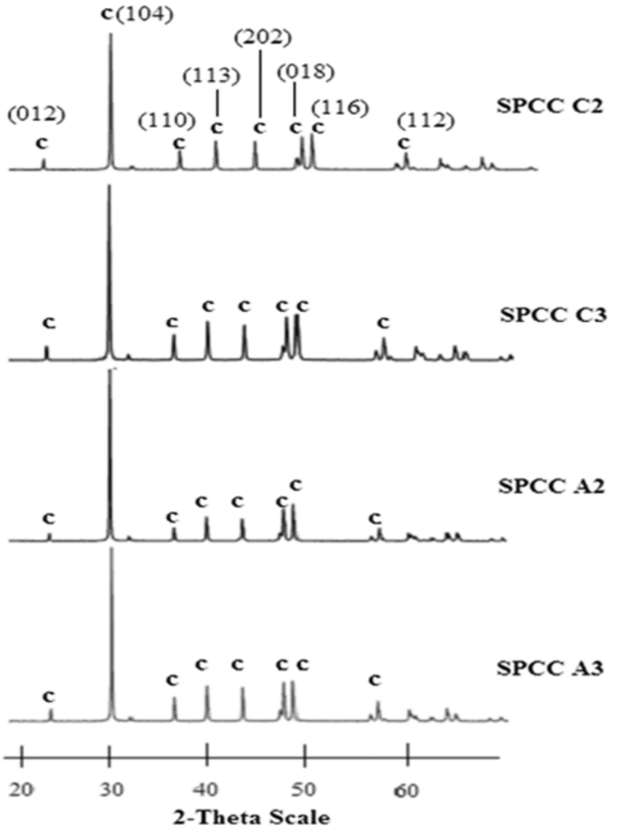

Fig. 5. XRD diffractogram showing calcite in all the sample peaks.

curately as the pattern allowed. The correct indices can be assigned to every line to the calcite pattern by using EVA analytical software (a universal software use to evaluate X-ray diffraction data).

Calcite, $CaCO_3$ has a hexagonal crystal structure, a space group R-3c, a punctual group of symmetry -32/m with lattice constants of a=b=4.990 Å, c=17.061 Å, α=β=90° and γ= 120° [23]. Fig. 5 shows the XRD pattern of a sample of calcite as prepared by the method described above. All the samples show almost similar peak position and intensity. It was compared with the data from EVA software, and all peaks of the obtained product can be assigned to those of calcite crystals, indicating the formation of single-phase calcite. Although there are no shifts in peak positions, the sharpness, and intensities of XRD lines have a little difference among these three calcites. For all samples used, the strongest diffraction intensity is the peak, which is a characteristic of calcite crystal lattice.

CONCLUSION

Spray mist technique hinted at an appreciable decrease of carbonation time and the process can be carried out continuously. This is because the spray mist increased reactant surface areas which sped up the reaction process and as a result, it allowed calcium carbonate (PCC) to precipitate immediately with specific morphology. From the SEM observation, the morphologies of PCC samples showed that the major view particle structures were twinned rhombohedral calcite. On the other hand, calcite is the only $CaCO_3$ polymorph obtained by this technique based on XRD and FTIR results. This technique is indeed a promising solution to improve industrial efficiency in PCC production with specific morphology with reduced lag time.

ACKNOWLEDGEMENT

The Authors sincerely wish to thank everyone whose assistance made this effort become a reality, especially to the technical staff of the School of Materials and Mineral Resources Engineering.

REFERENCES

1. K. Roy, M. N. Alam, S. K. Mandal and S. C. Debnath, *J. Nanostructure in Chemistry*, **6**, 15 (2016).
2. M. S. Nasser, M. J. Al-Marri, A. Benamor, S. A. Onaizi, M. Khraisheh and M. A. Saad, *Korean J. Chem. Eng.*, **33**, 448 (2016).
3. S. G. Lyu, S. Park and G. S. Sur, *Korean J. Chem. Eng.*, **16**, 538 (1999).
4. W. K. Park, S.-J. Ko, S. W. Lee, K.-H. Cho, J.-W. Ahn and C. Han, *J. Cryst. Growth*, **310**, 2593 (2008).
5. A.-R. Ibrahim, J. Vuningoma, Y. Huang, H. Wang and J. Li, *International J. Molecular Sciences*, **15**, 11350 (2014).
6. G. Montes-Hernandez, D. Daval, R. Chiriac and F. Renard, *Crystal Growth Design*, **10**, 4823 (2010).
7. D. J. Hwang, K. H. Cho, M. K. Choi, Y. H. Yu, S. K. Lee, J. W. Ahn, G. I. Lim, C. Han and J. D. Lee, *Korean J. Chem. Eng.*, **28**, 1927 (2011).
8. J.-H. Kim, S. M. Song, J. M. Kim, W. S. Kim and I. H. Kim, *Korean J. Chem. Eng.*, **27**, 1532 (2010).
9. M. Stroescu, A. Stoica-Guzun, S. I. Jinga, T. Dobre, I. M. Jipa and L. M. Dobre, *Korean J. Chem. Eng.*, **29**, 1216 (2012).
10. S. M. Song and I. H. Kim, *Korean J. Chem. Eng.*, **28**, 1749 (2011).
11. S. Satchawan, W. Naksata, C. Rattanakawin, S. Thiansem, P. Panya, P. Sooksamiti, P. J. Scales and O.-a. Arqueropanyo, *Korean J. Chem. Eng.*, **31**, 1076 (2014).
12. D. Chakraborty, V. Agarwal, S. Bhatia and J. Bellare, *Ind. Eng. Chem. Res.*, **33**, 2187 (1994).
13. B. Feng, A. K. Yong and H. An, *Mater. Sci. Eng.: A*, **445**, 170 (2007).
14. L. Xiang, Y. Xiang, Y. Wen and F. Wei, *Mater. Lett.*, **58**, 959 (2004).
15. F. A. Morsy, S. M. El-Sheikh and A. Barhoum, *Arabian J. Chemistry* (2014), DOI:10.1016/j.arabjc.2014.11.032.
16. M. Ukrainczyk, J. Kontrec and D. Kralj, *J. Colloid Interface Sci.*, **329**, 89 (2009).
17. T. Thenepalli, A. Jun, C. Han, C. Ramakrishna and J. Ahn, *Korean J. Chem. Eng.*, **32**, 1009 (2015).
18. D. Gómez-Díaz, J. M. Navaza and B. Sanjurjo, *Chem. Eng. J.*, **116**, 203 (2006).
19. B. Feng, A. K. Yong and H. An, *Mater. Sci. Eng.: A*, **445-446**, 170 (2007).
20. J.-W. Ahn, J.-H. Kim, H.-S. Park, J.-A. Kim, C. Han and H. Kim, *Korean J. Chem. Eng.*, **22**, 852 (2005).
21. K. Kim, H. Kim, C. Kim and J. Song, *Korean J. Chem. Eng.*, **33**(5), 1612 (2016).
22. C. K. Lee, *Appl. Surf. Sci.*, **202**, 15 (2002).
23. E. Zolotoyabko, E. Caspi, J. Fieramosca, R. Von Dreele, F. Marin, G. Mor, L. Addadi, S. Weiner and Y. Politi, *Cryst. Growth Design*, **10**, 1207 (2010).